Protein-protein interaction domains of Bacillus subtilis DivIVA

van Baarle, S.; Celik, I.N.; Kaval, K.G.; Bramkamp, M.; Hamoen, L.W.; Halbedel, S.

DOI
10.1128/JB.02171-12

Publication date
2013

Document Version
Final published version

Published in
Journal of Bacteriology

JB
Journals.ASM.org

Protein-Protein Interaction Domains of *Bacillus subtilis* DivIVA

Suey van Baarle,[b,c] Ilkay Nazli Celik,[b] Karan Gautam Kaval,[a] Marc Bramkamp,[c,d] Leendert W. Hamoen,[b,e] Sven Halbedel[a,b]

Robert Koch Institute, FG11—Division of Bacterial Infections, Wernigerode, Germany[a]; Centre for Bacterial Cell Biology, Newcastle University, Newcastle upon Tyne, United Kingdom[b]; Institute for Biochemistry, University of Cologne, Cologne, Germany[c]; Department Biology I, Ludwig-Maximilians University Munich, Biozentrum, Martinsried, Germany[d]; Bacterial Cell Biology, Swammerdam Institute for Life Sciences (SILS), University of Amsterdam, Amsterdam, The Netherlands[e]

DivIVA proteins are curvature-sensitive membrane binding proteins that recruit other proteins to the poles and the division septum. They consist of a conserved N-terminal lipid binding domain fused to a less conserved C-terminal domain. DivIVA homologues interact with different proteins involved in cell division, chromosome segregation, genetic competence, or cell wall synthesis. It is unknown how DivIVA interacts with these proteins, and we used the interaction of *Bacillus subtilis* DivIVA with MinJ and RacA to investigate this. MinJ is a transmembrane protein controlling division site selection, and the DNA-binding protein RacA is crucial for chromosome segregation during sporulation. Initial bacterial two-hybrid experiments revealed that the C terminus of DivIVA appears to be important for recruiting both proteins. However, the interpretation of these results is limited since it appeared that C-terminal truncations also interfere with DivIVA oligomerization. Therefore, a chimera approach was followed, making use of the fact that *Listeria monocytogenes* DivIVA shows normal polar localization but is not biologically active when expressed in *B. subtilis*. Complementation experiments with different chimeras of *B. subtilis* and *L. monocytogenes* DivIVA suggest that MinJ and RacA bind to separate DivIVA domains. Fluorescence microscopy of green fluorescent protein-tagged RacA and MinJ corroborated this conclusion and suggests that MinJ recruitment operates via the N-terminal lipid binding domain, whereas RacA interacts with the C-terminal domain. We speculate that this difference is related to the cellular compartments in which MinJ and RacA are active: the cell membrane and the cytoplasm, respectively.

DivIVA homologues constitute a group of highly conserved cell division proteins in Gram-positive bacteria. They bind to the cytosolic face of the cytoplasmic membrane and accumulate at membrane regions with increased negative curvature in rod-shaped bacteria (1–3). Negatively curved (i.e., concave) membrane regions occur at the cell poles and along the cytokinetic ring as soon as it starts to constrict and invaginates the cell membrane. Membrane binding and curvature sensitivity appear to be intrinsic features of DivIVA, as it was shown that DivIVA of *Bacillus subtilis* also localizes to curved membranes when expressed in other, nonrelated species, including yeast cells (4). DivIVA is used as a scaffold and recruits other proteins that function in cell division, cell wall biosynthesis, secretion, genetic competence, or chromosome segregation (5–13). The proteins that interact with DivIVA are therefore diverse and comprise both transmembrane and cytosolic proteins (14). The best-characterized DivIVA protein is that of *B. subtilis*, for which four different interaction partners are known: (i) the transmembrane protein MinJ, which acts as a molecular bridge between DivIVA and the FtsZ-inhibiting MinCD complex (11, 12); (ii) the DNA-binding protein RacA, which is required for chromosome segregation during spore formation (8, 15); (iii) the competence-specific inhibitor of cell division Maf (16); and (iv) the competence regulator ComN (17). Nothing is known about the molecular interaction between DivIVA and its interaction partners. We set out to determine DivIVA interaction domains in more detail and focused on the binding of *B. subtilis* DivIVA with MinJ and RacA.

The crystal structure of *B. subtilis* DivIVA revealed a two-domain organization: a highly conserved N-terminal domain that forms a dimeric structure with a characteristic cap structure and a less conserved C-terminal domain that is rich in coiled coils but varies in length among the different bacterial species (18). These domains are connected by a flexible ~20-amino-acid linker (Fig. 1). The N-terminal domain is required for the lipid binding of DivIVA and for localization (1, 18, 19). The dimeric cap structure of this lipid binding domain (LBD) exposes two phenylalanine side chains (F17, one per subunit), and the insertion of these side chains into the hydrophobic core of the phospholipid bilayer is essential for lipid binding (18). This membrane interaction is stabilized by auxiliary electrostatic interactions between positively charged arginine and lysine residues (R18 and K15) in the immediate vicinity of F17 and the negatively charged phospholipid head groups (18). The crystal structure suggested that the central coiled-coil region of the C-terminal domain contributes to DivIVA dimerization (Fig. 1B) and that the end of this domain (amino acids 130 to 153) forms an antiparallel four-helix bundle constituting the tetramerization domain (TD) whereby two DivIVA dimers are linked together in an end-to-end orientation (18) (Fig. 1A and B). The C-terminal part of DivIVA is the least-conserved domain; it differs in length and can contain large insertions (Fig. 1A). It was therefore speculated that this domain is responsible for the interaction with other proteins (14).

To test whether the C terminus of DivIVA comprises the partner interaction domain, we tested C-terminally truncated variants of *B. subtilis* DivIVA for their interaction with MinJ and RacA using the bacterial two-hybrid system. These experiments proved inconclusive since removal of the tetramerization domain ap-

Received 29 November 2012 Accepted 14 December 2012
Published ahead of print 21 December 2012
Address correspondence to Sven Halbedel, halbedels@rki.de, or Leendert W. Hamoen, l.w.hamoen@uva.nl.
Supplemental material for this article may be found at http://dx.doi.org/10.1128/JB.02171-12.

doi:10.1128/JB.02171-12

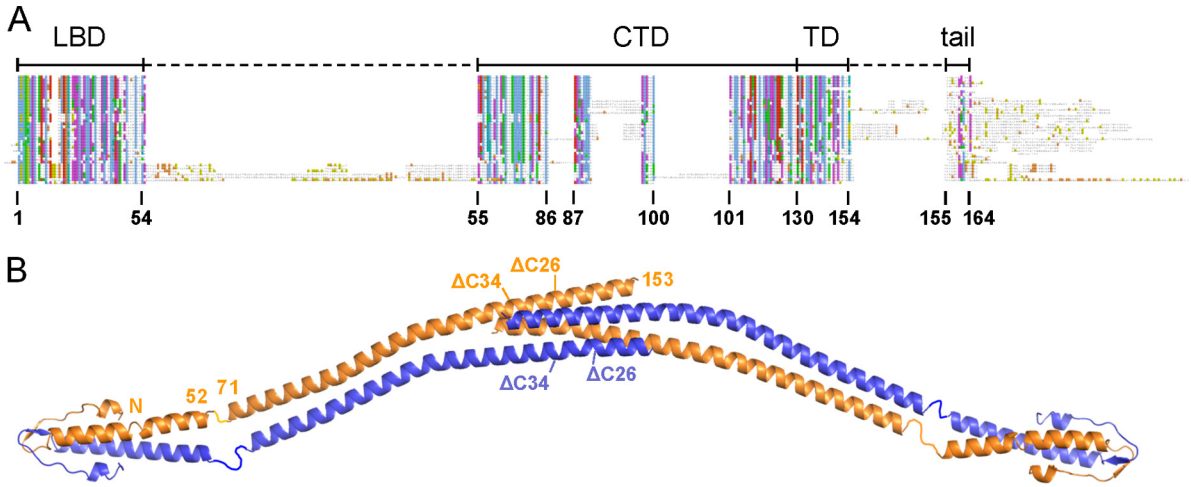

FIG 1 Domain arrangement of *B. subtilis* DivIVA. (A) Schematic sequence alignment of DivIVA proteins of different phylogenetic origins. Abbreviations above the alignment label the individual protein regions: LBD, lipid binding domain; CTD, C-terminal domain; TD, tetramerization domain; tail, C-terminal tail region. Amino acid numbering is according to the *B. subtilis* DivIVA sequence. (B) Model of the crystal structure of the full-length *B. subtilis* DivIVA tetramer which has been assembled from the individual crystal structures of the N- and the C-terminal domains (18). Crystallographic data for the linker between both domains (residues 53 to 70) are not available. Amino acid positions at the beginning and the end of the lipid binding domain as well as the C-terminal domain are indicated for one molecule. Truncation sites of DivIVAΔC26 and DivIVAΔC34 at positions 138 and 130, respectively, are also shown (compare Table 3).

peared to affect oligomerization. Therefore, we set up a complementation assay with chimeric DivIVA proteins that consist of domains from *B. subtilis* DivIVA and *Listeria monocytogenes* DivIVA. The latter protein localizes normally when expressed in *B. subtilis* but is biologically inactive and is unable to recruit MinJ or RacA to the cell division sites and cell poles. This experiment revealed that the sporulation activity and the cell division activity of DivIVA can be separated. It emerged that the transmembrane protein MinJ binds to the N-terminal lipid binding domain of DivIVA, whereas the C-terminal domain of DivIVA contains the binding site for the cytosolic protein RacA.

MATERIALS AND METHODS

Bacterial strains and growth conditions. All bacterial strains that were used in this study are listed in Table 1. Routinely, *B. subtilis* strains were cultivated in LB broth or on LB agar at 37°C. If necessary, the following antibiotics were added at the indicated concentrations: tetracycline (10 μg/ml), spectinomycin (100 μg/ml), and chloramphenicol (5 μg/ml). Other supplements were IPTG (isopropyl-β-D-thiogalactopyranoside; 1 mM) and xylose (0.5%). For all cloning procedures, *Escherichia coli* TOP10 was used as the standard plasmid host (23).

Construction of bacterial two-hybrid plasmids. In order to construct C-terminal truncations of *divIVA* for use in the bacterial two-hybrid assay, plasmids p25N-*divIVA* and pUT18-*divIVA* were used as the templates in a PCR with oligonucleotide 25_N_18_F as the forward primer and the oligonucleotides *divIVA*_11_B2H_R (DivIVA which lacks the last 11 C-terminal amino acids [DivIVAΔ11]), *divIVA*_19_B2H_R (DivIVAΔ20), *divIVA*_21_R (DivIVAΔ21), *divIVA*_26_R (DivIVAΔ26), and *divIVA*_34_R (DivIVAΔ34) as the complementary primers (for all primer sequences, see Table 2). The PCR products were KpnI digested, self-ligated, and transformed to *E. coli*. The appropriate clones were identified using restriction analysis and DNA sequencing.

Construction of plasmids containing *divIVA* from *B. subtilis* and *L. monocytogenes*. For xylose-inducible expression of *B. subtilis divIVA* (*divIVA*^{Bs}), we constructed plasmid pSH19. This plasmid was obtained by introducing a stop codon between *divIVA* and *gfp* using plasmid pSH3 as the template and the oligonucleotides SV23/SV24 as the primers in a QuikChange mutagenesis reaction. In order to express the *L. monocytogenes divIVA* (*divIVA*^{Lm}) gene in *B. subtilis* cells, plasmid pSH209 was constructed. This plasmid contains the complete *lmo2020* open reading frame of *L. monocytogenes* under the control of the P_{xyl} promoter. It was obtained by amplification of the *L. monocytogenes divIVA* DNA fragment with the oligonucleotides SHW109/SHW110 and subsequent cloning of the obtained fragment into plasmid pSG1154 using KpnI/XhoI. Plasmid pSH210 was constructed in the same way to allow the expression of *L. monocytogenes* DivIVA-green fluorescent protein (GFP) in cells of *B. subtilis*. However, for this cloning, the *divIVA* DNA fragment was amplified with primers SHW109/SHW111 to fuse the *divIVA* gene in frame to the *gfp* gene of the vector backbone. The A206K mutation, which prevents dimerization of GFP (24, 25), was introduced into the *gfp* part of plasmid pSH210 using QuikChange mutagenesis with SHW425/SHW426 as the mutagenic primers. The resulting plasmid was sequenced and named pSH354.

Construction of *divIVA* chimeras. For the construction of chimeric *divIVA* genes consisting of N-terminal parts from *L. monocytogenes* and C-terminal parts from *B. subtilis*, a PCR-based restriction-free cloning strategy was used (26). C-terminal fragments of the *B. subtilis divIVA* gene were amplified from plasmid pSH19 with SHW237 (pSH260), SHW238 (pSH261), SHW247 (pSH267), SHW265 (pSH272), and SHW266 (pSH278) as the respective forward primers and SHW184 as the reverse primer in a first step. All forward primers were identical to the desired fusion sites in the *L. monocytogenes divIVA* gene in their 5′ regions, whereas the reverse primer SHW184 annealed outside the *B. subtilis divIVA* gene in the pSH19 plasmid backbone. For the construction of the *divIVA*$^{Bs\text{-}57\text{-}Lm}$ chimera, a DNA fragment corresponding to the first 57 amino acids of the *B. subtilis divIVA* gene was amplified in a PCR with pSH19 as the template and SHW354 and SHW355 as the primers. All PCR products were purified using a PCR purification kit from Qiagen and used as megaprimers in a second PCR with plasmid pSH209 as the template in order to fuse the N- and C-terminal fragments of *B. subtilis divIVA* to the corresponding portions of the *L. monocytogenes divIVA* gene. For the construction of the *divIVA*$^{Bs\text{-}57\text{-}Lm}$ chimera (pKK13), primer SHW180 was added as a reverse primer to the PCR mixture. The PCR mixtures were then DpnI digested and transformed, and the correct clones were identified using restriction analysis and DNA sequencing.

GFP was fused to all DivIVA chimeras by replacing the stop codon of the chimeric *divIVA* genes by a glycine codon in a way in that the *divIVA*

TABLE 1 Plasmids and strains used in this study

Plasmid or strain	Relevant characteristic	Source or reference
Plasmids		
pAPNC213	*bla aprE5′ spc lacI* P_{spac} *aprE3′*	20
pAPNC213cat	*bla aprE5′ cat lacI* P_{spac} *aprE3′*	H. Strahl
pDG9	*bla amyE3′ spc* P_{xyl}*-divIVA-gfp amyE5′*	18
pSG1154	*bla amyE3′ spc* P_{xyl}*-′gfp amyE5′*	21
pSH2	*bla aprE5′ spc lacI* P_{spac}*-divIVA*^{Bs} *aprE3′*	18
pSH3	*bla amyE3′ spc* P_{xyl}*-divIVA*^{Bs}*-gfpA206K amyE5′*	18
pKT25-*racA*	*kan* P_{lac}*-cya*(T25)*-racA*	1
pUT18-*divIVA*	*bla* P_{lac}*-cya*(T18)*-divIVA*	1
pUT18C-*divIVA*	*bla* P_{lac}*-cya*(T18)*-divIVA*	11
pUT18C-*minJ*	*bla* P_{lac}*-cya*(T18)*-minJ*	11
pUT18C-*racA*	*bla* P_{lac}*-cya*(T18)*-racA*	1
p25-N-*divIVA*	*kan* P_{lac}*-divIVA-cya*(T25)	1
p25-N-*minJ*	*kan* P_{lac}*-minJ-cya*(T25)	11
pINC3	*bla amyE3′ spc* P_{xyl}*-divIVAR131A-gfp amyE5′*	This work
pINC12	*bla aprE5′ spc lacI* P_{spac}*-divIVAR131A aprE3′*	This work
pKK13	*bla amyE3′ spc* P_{xyl}*-divIVA*$^{Bs\text{-}57\text{-}Lm}$ *amyE5′*	This work
pSBLH001	*bla* P_{lac}*-divIVA*$^{1\text{-}459}$(Δ11)*-cya*(T18)[a]	This work
pSBLH004	*kan* P_{lac}*-divIVA*$^{1\text{-}459}$(Δ11)*-cya*(T25)	This work
pSBLH005	*bla* P_{lac}*-divIVA*$^{1\text{-}432}$(Δ20)*-cya*(T18)	This work
pSBLH008	*kan* P_{lac}*-divIVA*$^{1\text{-}432}$(Δ20)*-cya*(T25)	This work
pSBLH036	*bla* P_{lac}*-divIVA*$^{1\text{-}429}$(Δ21)*-cya*(T18)	This work
pSBLH037	*bla* P_{lac}*-divIVA*$^{1\text{-}414}$(Δ26)*-cya*(T18)	This work
pSBLH038	*bla* P_{lac}*-divIVA*$^{1\text{-}390}$(Δ34)*-cya*(T18)	This work
pSBLH039	*kan* P_{lac}*-divIVA*$^{1\text{-}429}$(Δ21)*-cya*(T25)	This work
pSBLH040	*kan* P_{lac}*-divIVA*$^{1\text{-}414}$(Δ26)*-cya*(T25)	This work
pSBLH041	*kan* P_{lac}*-divIVA*$^{1\text{-}390}$(Δ34)*-cya*(T25)	This work
pSH19	*bla amyE3′ spc* P_{xyl}*-divIVA*^{Bs} *amyE5′*	This work
pSH209	*bla amyE3′ spc* P_{xyl}*-divIVA*^{Lm} *amyE5′*	This work
pSH210	*bla amyE3′ spc* P_{xyl}*-divIVA*^{Lm}*-gfp amyE5′*	This work
pSH260	*bla amyE3′ spc* P_{xyl}*-divIVA*$^{Lm\text{-}71\text{-}Bs}$ *amyE5′*	This work
pSH261	*bla amyE3′ spc* P_{xyl}*-divIVA*$^{Lm\text{-}144\text{-}Bs}$ *amyE5′*	This work
pSH267	*bla amyE3′ spc* P_{xyl}*-divIVA*$^{Lm\text{-}130\text{-}Bs}$ *amyE5′*	This work
pSH272	*bla amyE3′ spc* P_{xyl}*-divIVA*$^{Lm\text{-}83\text{-}Bs}$ *amyE5′*	This work
pSH278	*bla amyE3′ spc* P_{xyl}*-divIVA*$^{Lm\text{-}104\text{-}Bs}$ *amyE5′*	This work
pSH290	*bla amyE3′ spc* P_{xyl}*-divIVA*$^{Lm\text{-}71\text{-}Bs}$*-gfpA206K amyE5′*	This work
pSH291	*bla amyE3′ spc* P_{xyl}*-divIVA*$^{Lm\text{-}144\text{-}Bs}$*-gfpA206K amyE5′*	This work
pSH292	*bla amyE3′ spc* P_{xyl}*-divIVA*$^{Lm\text{-}130\text{-}Bu}$*-gfpA206K amyE5′*	This work
pSH293	*bla amyE3′ spc* P_{xyl}*-divIVA*$^{Lm\text{-}83\text{-}Bs}$*-gfpA206K amyE5′*	This work
pSH294	*bla amyE3′ spc* P_{xyl}*-divIVA*$^{Lm\text{-}104\text{-}Bs}$*-gfpA206K amyE5′*	This work
pSH316	*bla aprE5′ cat lacI* P_{spac}*-minJ-gfp aprE3′*	This work
pSH317	*bla aprE5′ cat* P_{spac}*-minJ-gfp aprE3′*	This work
pSH320	*bla aprE5′ cat* $P_{divIVA1}$*-minJ-gfp aprE3′*	This work
pSH326	*bla amyE3′ spc* P_{xyl}*-divIVA*$^{Bs\text{-}57\text{-}lm}$*-gfp amyE5′*	This work
pSH328	*bla aprE5′ cat* $P_{divIVA3}$*-minJ-gfp aprE3′*	This work
pSH330	*bla aprE5′ spc lacI* P_{spac}*-divIVA*^{Bs}*R102K aprE3′*	This work
pSH331	*bla aprE5′ spc lacI* P_{spac}*-divIVA*^{Bs}*R102E aprE3′*	This work
pSH334	*bla aprE5′ spc lacI* P_{spac}*-divIVA*^{Bs}Δ*C34 aprE3′*	This work
pSH335	*bla aprE5′ cat lacI* P_{spac}*-divIVA*^{Bs} *aprE3′*	This work
pSH336	*bla aprE5′ cat lacI* P_{spac}*-divIVA*^{Bs}*R102K aprE3′*	This work
pSH337	*bla aprE5′ cat lacI* P_{spac}*-divIVA*^{Bs}*R102E aprE3′*	This work
pSH340	*bla aprE5′ cat lacI* P_{spac}*-divIVA*^{Bs}Δ*C34 aprE3′*	This work
pSH354	*bla amyE3′ spc* P_{xyl}*-divIVA*^{Lm}*-gfpA206K amyE5′*	This work
pSH355	*bla amyE3′ spc* P_{xyl}*-divIVA*$^{Bs\text{-}57\text{-}Lm}$*-gfpA206K amyE5′*	This work

TABLE 1 (Continued)

Plasmid or strain	Relevant characteristic	Source or reference
B. subtilis strains		
168	*trpC2*	
168(pSG4916)	168 *racA*::pSG4916(P_{xyl}*-gfp-racA′ cat*)	8
4041	168 *divIVA::tet*	18
BSN5	168 *aprE*::P_{spac}*-divIVA spc lacI divIVA::tet*	18
SB002	168 *amyE*::P_{xyl}*-minJ-gfp spc minJ::tet*	22
BSN51	168 *amyE*::P_{xyl}*-divIVA*^{Bs} *spc divIVA::tet*	This work
BSN238	168 *amyE*::P_{xyl}*-divIVA*^{Lm} *spc divIVA::tet*	This work
BSN274	168 *amyE*::P_{xyl}*-divIVA*$^{Lm\text{-}144\text{-}Bs}$ *spc divIVA::tet*	This work
BSN278	168 *amyE*::P_{xyl}*-divIVA*$^{Lm\text{-}130\text{-}Bs}$ *spc divIVA::tet*	This work
BSN287	168 *amyE*::P_{xyl}*-divIVA*$^{Lm\text{-}83\text{-}Bs}$ *spc divIVA::tet*	This work
BSN288	168 *amyE*::P_{xyl}*-divIVA*$^{Lm\text{-}104\text{-}Bs}$ *spc divIVA::tet*	This work
BSN294	168 *amyE*::P_{xyl}*-divIVA*$^{Lm\text{-}71\text{-}Bs}$*-gfpA206K spc divIVA::tet*	This work
BSN295	168 *amyE*::P_{xyl}*-divIVA*$^{Lm\text{-}144\text{-}Bs}$*-gfpA206K spc divIVA::tet*	This work
BSN296	168 *amyE*::P_{xyl}*-divIVA*$^{Lm\text{-}130\text{-}Bs}$*-gfpA206K spc divIVA::tet*	This work
BSN297	168 *amyE*::P_{xyl}*-divIVA*$^{Lm\text{-}83\text{-}Bs}$*-gfpA206K spc divIVA::tet*	This work
BSN298	168 *amyE*::P_{xyl}*-divIVA*$^{Lm\text{-}104\text{-}Bs}$*-gfpA206K spc divIVA::tet*	This work
BSN308	168 *aprE*::P_{spac}*-minJ-gfp cat lacI*	This work
BSN313	168 *aprE*::P_{spac}*-divIVAR131A spc lacI divIVA::tet*	This work
BSN316	168 *amyE*::P_{xyl}*-divIVA*$^{Lm\text{-}71\text{-}Bs}$ *spc divIVA::tet*	This work
BSN317	168 *aprE*::P_{spac}*-minJ-gfp cat*	This work
BSN321	168 *amyE*::P_{xyl}*-divIVA*$^{Bs\text{-}57\text{-}Lm}$ *spc divIVA::tet*	This work
BSN332	168 *aprE*::$P_{divIVA3}$*-minJ-gfp cat*	This work
BSN333	168 *aprE*::$P_{divIVA3}$*-minJ-gfp cat divIVA::tet*	This work
BSN334	168 *aprE*::$P_{divIVA3}$*-minJ-gfp cat amyE*::P_{xyl}*-divIVA*^{Bs} *spc divIVA::tet*	This work
BSN335	168 *aprE*::$P_{divIVA3}$*-minJ-gfp cat amyE*::P_{xyl}*-divIVA*^{Lm} *spc divIVA::tet*	This work
BSN336	168 *aprE*::$P_{divIVA3}$*-minJ-gfp cat amyE*::P_{xyl}*-divIVA*$^{Lm\text{-}104\text{-}Bs}$ *spc divIVA::tet*	This work
BSN338	168 *aprE*::$P_{divIVA3}$*-minJ-gfp cat amyE*::P_{xyl}*-divIVA*$^{Bs\text{-}57\text{-}Lm}$ *spc divIVA::tet*	This work
BSN340	168 *racA*::pSG4916(P_{xyl}*-gfp-racA′ cat*) *amyE*::P_{xyl}*-divIVA*^{Bs} *spc divIVA::tet*	This work
BSN341	168 *racA*::pSG4916(P_{xyl}*-gfp-racA′ cat*) *amyE*::P_{xyl}*-divIVA*^{Lm} *spc divIVA::tet*	This work
BSN342	168 *racA*::pSG4916(P_{xyl}*-gfp-racA′ cat*) *amyE*::P_{xyl}*-divIVA*$^{Lm\text{-}104\text{-}Bs}$ *spc divIVA::tet*	This work
BSN344	168 *racA*::pSG4916(P_{xyl}*-gfp-racA′ cat*) *amyE*::P_{xyl}*-divIVA*$^{Bs\text{-}57\text{-}Lm}$ *spc divIVA::tet*	This work
BSN356	168 *aprE*::P_{spac}*-divIVA*^{Bs} *cat lacI divIVA::tet*	This work
BSN357	168 *aprE*::P_{spac}*-divIVA*^{Bs}*R102K cat lacI divIVA::tet*	This work
BSN358	168 *aprE*::P_{spac}*-divIVA*^{Bs}*R102E cat lacI divIVA::tet*	This work
BSN360	168 *aprE*::P_{spac}*-divIVA*^{Bs}Δ*C34 cat lacI divIVA::tet*	This work
BNS372	168 *amyE*::P_{xyl}*-divIVA*$^{Bs\text{-}57\text{-}Lm}$*-gfpA206K spc divIVA::tet*	This work
BSN373	168 *amyE*::P_{xyl}*-divIVA*^{Lm}*-gfpA206K spc divIVA::tet*	This work

[a] The designations represent, e.g., for *divIVA*$^{1\text{-}459}$(Δ11), *divIVA* from nucleotide positions 1 to 459 with a deletion of the 11 C-terminal amino acid residues.

genes were fused to the downstream *gfp* open reading frame that was already present in these plasmids. For this purpose, we used the oligonucleotides SHW304/SHW305 to replace the *divIVA* stop codons in plasmids pSH260, pSH261, pSH267, pSH272, and pSH278. The replacement

TABLE 2 Oligonucleotides used in this study

Name	Sequence (5′ → 3′)
25_N_18_F	CCGGGTACCGAGCTCGAATTCA
*divIVA*_11_B2H_R	GCGGGTACCTCAAGGAGATGATCCCA
*divIVA*_19_B2H_R	GCGGGTACCAATTTCAGAAGATCAAG
*divIVA*_21_R	GCGGGTACCAGAAGATCAAGCTGAGCT
*divIVA*_26_R	GCGGGTACCGCTTCAATCAGCATTTGG
*divIVA*_34_R	GCGGGTACCGTTCTGAACACTTTAGAC
SHW109	CTTAGGTACCAAGCTAGTAACTATGGTAGAATG
SHW110	GCGCTCGAGTTAACGTTCTTCAGATTCAGCTG
SHW111	GCGCTCGAGACGTTCTTCAGATTCAGCTG
SHW180	CGAAGTAAATGACTTCCTCGATC
SHW184	CTTAACTAGTTTTGTATAGTTCATCCATGCC
SHW237	GAACGTTTAGGTCATTTTACAAACATTGAGGAGA CATTGAATAAATC
SHW238	GTGGAAGCACAAATGGATTTAATTAAAAATGACG ATTGGGATCATC
SHW247	CGTCAATCCAAAGTATTCCGTACACGTTTCCAAA TGCTGATTG
SHW265	CAAACAGCTGCCGAAGAAGTGAAACGCAATTCTC AAAAAGAAGCAAAG
SHW266	GCAGAAAAAAATGCTGACCGAATTATCAACGAAT CGTTATCAAAATC
SHW304	AAAGGAAGGACTTGATATCGAATTCC
SHW305	TATCAAGTCCTTCCTTTTCCTCAAATAC
SHW342	ATATGTCGACACATAAAATGCATCTAGAAAGGAG
SHW343	GCGCGGATCCTTATTTGTATAGTTCATCCATGCC
SHW349	TTGCGCTCACATCAAATCGTCTCCCTCCG
SHW350	GATTTGATGTGAGCGCAACGCAAGCTTC
SHW354	GTCGTATGGAGGTGCTAGATATGCCATTAACGCC AAATGATATTC
SHW355	GTTTCTTCAATGTTTGTAAAATGACCGATTCTTT CATCAAGCTCATTG
SHW356	GACACCTCGAGCATGATGCCACCTCCATTTTTAC
SHW357	TGATGCCACCTCCATTTTTACATTTC
SHW358	AAATGGAGGTGGCATCATGCTCGAGG
SHW366	GAAGAACGTGGACTCGAGGTCGACGGTATC
SHW367	GACCTCGAGTCCACGTTCTTCAGATTCAGCTG
SHW378	CGCTGATAAAATTATCAACGAATCG
SHW379	GATAATTTTATCAGCGTTTTTCTCC
SHW380	CGCTGATGAAATTATCAACGAATC
SHW381	GATAATTTCATCAGCGTTTTTCTCC
SHW386	TCAGAACATAATTCCAAATGCTGATTGAAG
SHW387	ATTTGGAATTATGTTCTGAACACTTTAGAC
SHW425	CACAATCTAAACTTTCCAAAGATCCCAACG
SHW426	GGAAAGTTTAGATTGTGTGGACAGGTAATG
SV23	GAAAAGGAATAACTTGATATCGAATTC
SV24	GATATCAAGTTATTCCTTTTCCTCAAATAC
SV81	CGCGCGAGCTCTTATTCCTTTTCCTCAAATACAGC
SV98	CTTAGGTACCTTGGCCGGTGCAGCTTAAC
SV123	CGGGATCCAAAATGGAGGTGGCATCATGCCATTA ACGCCAAATG
R131A_fw	TCAGAACAGCTTTCCAAATGCTGATTG
R131A_rev	TTTGGAAAGCTGTTCTGAACACTTTAG

of the *divIVA* stop codon in plasmid pKK13 was performed using the primer pair SHW366/SHW367. The DNA sequences of all plasmid clones were verified, and the plasmids were named pSH290 (*divIVA*$^{Lm\text{-}71\text{-}Bs}$-*gfpA206K*, where *gfpA206K* represents the A-to-K change at position 206 encoded by *gfp*), pSH291 (*divIVA*$^{Lm\text{-}144\text{-}Bs}$-*gfpA206K*), pSH292 (*divIVA*$^{Lm\text{-}130\text{-}Bs}$-*gfpA206K*), pSH293 (*divIVA*$^{Lm\text{-}83\text{-}Bs}$-*gfpA206K*), pSH294 (*divIVA*$^{Lm\text{-}104\text{-}Bs}$-*gfpA206K*), and pSH326 (*divIVA*$^{Bs\text{-}57\text{-}Lm}$-*gfp*). Finally, the *gfpA206K* mutation was also introduced into plasmid pSH326 as described above to result in plasmid pSH355.

Construction of a *minJ-gfp* fusion. In order to express a *minJ-gfp* fusion in the *divIVA* chimera strains, the *minJ-gfp* allele of strain SB002 was PCR amplified using the oligonucleotides SHW342/SHW343, the resulting PCR fragment was cut with BamHI/SalI and ligated to pAPNC213cat digested with the same enzymes, and the resulting plasmid was named pSH316 after DNA sequencing. However, there was only marginal MinJ-GFP fluorescence, when pSH316 was inserted into the *B. subtilis* chromosome under inducing conditions (strain BSN308; data not shown). Therefore, plasmid pSH317 was constructed, in which the *lacI* gene of pSH316 was deleted by PCR using the primer pair SHW349/SHW350 in order to enhance the fluorescence signal. MinJ-GFP fluorescence was still not sufficient with this allele (strain BSN317; data not shown), so the promoter region of the *B. subtilis divIVA* gene, including the ribosomal binding site (RBS), was amplified with primers SV98/SHW356, and the resulting PCR fragment was cut with KpnI and XhoI and ligated to pSH317, which had been cut with the same enzymes. Two clones that contained a *divIVA* promoter insert of the right size were isolated, but DNA sequencing revealed single mutations in the RBS ($P_{divIVA1}$ on pSH320). In order to correct this, QuikChange mutagenesis with primers SHW357/SHW358 was employed on pSH320, and several plasmid clones were isolated and transformed to *B. subtilis*. From these transformations, only three plasmid clones conferred the typical fluorescence pattern of MinJ-GFP on cells of *B. subtilis*. When sequenced, one of these clones had a corrected RBS but also an unintended G deletion between the RBS and the MinJ-GFP start codon ($P_{divIVA3}$). This clone was named pSH328 and used for all further studies.

Construction of point mutations and C-terminal truncations in *divIVA*. For the construction of plasmid pINC12 encoding the *divIVAR131A* gene (where *divIVAR131A* represents the R-to-A change at position 131 encoded by *divIVA*) under the control of the P_{spac} promoter, we made use of plasmid pINC3, which already contained the *divIVAR131A-gfp* allele. pINC3 was originally obtained by QuikChange mutagenesis using the mutagenesis primers R131A_fw/R131A_rev on plasmid pDG9. *divIVAR131A* of pINC3 was then amplified using the primers SV123/SV81, and the resulting PCR fragment was cut with BamHI/SalI and ligated to the BamHI/SalI-cut vector backbone of plasmid pAPNC213. The DNA sequence of one clone was verified, and this clone was named pINC12. The R102K, R102E, and ΔC34 (deletion of the C-terminal 34 amino acid residues) mutations were introduced into plasmid pSH2 by QuikChange mutagenesis using the oligonucleotides SHW378/SHW379 (pSH330), SHW380/SHW381 (pSH331), and SHW386/SHW387 (pSH334), respectively. In order to exchange the *spc* marker for a *cat* cassette in these plasmids, the KpnI/SacI P_{spac}-*divIVA* fragments of pSH2, pSH330, pSH331, and pSH334 were then subcloned into the KpnI/SacI-cut backbone of pAPNC213cat in a second step. The resulting plasmids were sequenced and named pSH335 (wild type [wt]), pSH336 (R102K), pSH337 (R102E), and pSH340 (ΔC34).

Strain construction. Plasmids designed for the expression of *divIVA* alleles in *B. subtilis* were inserted into the *amyE* gene of *B. subtilis* 168, and amylase-negative transformants were selected on the basis of iodine staining of starch-containing agar plates. Alternatively, the *aprE* locus was also used for chromosomal integrations. Insertions at *aprE* were generally confirmed by PCR. Combinations of alleles were generated by transformation (27).

Bacterial two-hybrid analysis. In order to investigate the interaction of the DivIVA and C-terminally truncated DivIVA proteins with MinJ and RacA, the bacterial two-hybrid system was used (28). Plasmids encoding *divIVA* alleles fused to the T18 or the T25 fragment of the *Bordetella pertussis* adenylate cyclase were cotransformed in *E. coli* BTH101 along with plasmids encoding T25 and T18 fusions to RacA and MinJ. Transformants were selected on nutrient agar plates containing ampicillin (100 μg/ml), kanamycin (50 μg/ml), X-Gal (5-bromo-4-chloro-3-indolyl-β-D-galactopyranoside; 0.004%), and IPTG (0.1 mM), and photographs were taken after 40 h of growth at 30°C.

TABLE 3 Bacterial two-hybrid analysis of C-terminal DivIVA truncation mutants regarding their ability to interact with full-length DivIVA, MinJ, and RacA

DivIVA	C-terminal protein sequence[a]	Reactivity[b]		
		DivIVA	MinJ	RacA
wt	LKKQSKVFRTRFQMLIEAQLDLLKNDDWDHLLEYEVDAVFEEKE-164	+	+	±
Δ11	LKKQSKVFRTRFQMLIEAQLDLLKNDDWDHLLE-153	+	+	−
Δ20	LKKQSKVFRTRFQMLIEAQLDLLK-144	+	+	−
Δ21	LKKQSKVFRTRFQMLIEAQLDLL-143	+	+	−
Δ26	LKKQSKVFRTRFQMLIEA-138	±	±	−
Δ34	LKKQSKVFRT-130	±	±	−

[a] Starting from position 121. The shadowed sequence stretch corresponds to the DivIVA tetramerization domain. The position of the last amino acid in the truncated DivIVA proteins is given at the end of the sequence.
[b] Symbols coincide with the colors in Fig. S1 in the supplemental material: +, dark blue; ±, light blue; −, white.

Microscopic techniques. For microscopy of bacterial cells, a small volume (0.3 μl) of an exponentially growing culture was mounted on a microscope slide covered with a thin film of 1.5% agarose (dissolved in distilled water). Membranes were stained using FM5-95. Images were taken with a Nikon Eclipse Ti microscope coupled to a Nikon DS-MBWc charge-coupled-device camera and processed using the NIS elements AR software package (Nikon).

Sporulation assays. *B. subtilis* strains were streaked on Schaeffer′s sporulation agar (29) containing 0.5% xylose or 1 mM IPTG and incubated for up to 7 days at 37°C, until lysis of the translucent sporulation-deficient strains could be comfortably discriminated from the optically dense appearance of sporulation-proficient strains. Plates were photographed against a black background.

Isolation of cellular proteins, PAGE techniques, and Western blotting. Exponentially growing cells of *B. subtilis* were harvested by centrifugation (13,000 rpm for 1 min in an Eppendorf 5415R tabletop centrifuge), and the cell pellet was washed once in ZAP buffer (10 mM Tris-HCl, pH 7.5, 200 mM NaCl). Cells were disrupted by sonication in ZAP buffer containing 1 mM phenylmethylsulfonyl fluoride, and cell debris was pelleted in another centrifuge run. Aliquots of the resulting supernatant were separated either by SDS-PAGE or by blue native PAGE, which was performed using NativePAGE Novex 4 to 16% bis-Tris gels (Invitrogen) and carried out according to the instructions given by the manufacturer. Subsequently, gels were blotted onto a polyvinylidene difluoride (PVDF) membrane employing a semidry electroblotting unit. Proteins of interest were visualized using polyclonal rabbit antisera recognizing DivIVA (5) or GFP (lab stock) as the primary antibodies and an anti-rabbit immunoglobulin G conjugated to horseradish peroxidase as the secondary one. An ECL chemiluminescence detection kit (Thermo Scientific) was then used for the detection of the peroxidase conjugates on the PVDF membranes.

RESULTS

C-terminal DivIVA truncations interfere with MinJ and RacA binding. The tetramerization domain of *B. subtilis* DivIVA is followed by 11 nonconserved amino acid residues. The atomic structure of this C-terminal stretch could not be solved using crystallography, suggesting that it is a flexible tail. To determine whether this C-terminal tail is involved in the binding of MinJ and/or RacA, we made use of the bacterial two-hybrid assay and cloned two DivIVA truncations in this system: DivIVAΔ11, which lacks the last 11 C-terminal amino acids, and DivIVAΔ20, which lacks the last 20 C-terminal amino acids, including a part of the tetramerization domain (Table 3). Both truncations were still able to interact with full-length DivIVA, indicating that both mutants are expressed normally and can form dimers (Table 3; a colored image of the bacterial two-hybrid plate is available in Fig. S1 in the supplemental material). MinJ interacted strongly with full-length DivIVA and with both DivIVA truncations in the bacterial two-hybrid assay, whereas RacA showed a weak interaction with full-length DivIVA that was abolished when the last 11 amino acids of DivIVA were removed (Table 3; see Fig. S1 in the supplemental material). It seems that the RacA-DivIVA interaction depends on the 11 C-terminal amino acids of DivIVA, whereas the MinJ contact site is located more to the N terminus of DivIVA. To test this, additional DivIVA truncations were constructed: DivIVAΔ21, DivIVAΔ26, and DivIVAΔ34. These truncations successively removed the complete tetramerization domain. The last two truncations, DivIVAΔ26 and DivIVAΔ34, were severely impaired in their ability to interact with MinJ (Table 3; see Fig. S1 in the supplemental material), suggesting that the tetramerization domain contains residues required for MinJ binding.

Importance of the tetramerization domain for DivIVA activity. The bacterial two-hybrid assay also revealed a weakened interaction of the DivIVAΔ26 (corresponding to DivIVA amino acids 1 to 138) and DivIVAΔ34 (corresponding to DivIVA amino acids 1 to 130) truncations with full-length DivIVA, whereas the DivIVAΔ21 truncation (corresponding to DivIVA amino acids 1 to 143) still behaved normally (Table 3; see Fig. S1 in the supplemental material). So far there is no biochemical corroboration that amino acids 130 to 143 are involved in tetramerization *in vivo*. Own preliminary alanine mutagenesis experiments in this region identified R131 as an essential residue for DivIVA activity (see Fig. S3A to C in the supplemental material), suggesting a special importance of this region for DivIVA function. Thus, DivIVAΔC34 was expressed in a Δ*divIVA* mutant (strain BSN360), and phenotypic analysis of this strain clearly demonstrated the inability of the *divIVAΔC34* allele to complement the cell division and the sporulation phenotype of the Δ*divIVA* mutation (Fig. 2A and B), even though DivIVAΔC34 was clearly expressed (Fig. 2C, top). Blue native PAGE of strain BSN356 expressing wild-type DivIVA showed that DivIVA exists in two different oligomeric states since two signals of different molecular masses were detected by the DivIVA antiserum (Fig. 2C, bottom). The molecular masses were calculated to be 159 ± 8 kDa for the upper signal and 41 ± 13 kDa for the lower signal in the wild-type cell extract. Given the molecular mass of *B. subtilis* DivIVA (19.34 kDa), these molecular masses correspond to an octamer and a dimer, respectively. Blue native PAGE of strain BSN360 revealed the existence of a dimer signal (Fig. 2C, bottom). Previous gel filtration analyses have indicated that purified DivIVA forms octamers and higher-order structures (18, 30). Therefore, it seems plausible that the region beyond residue 130 indeed contains the

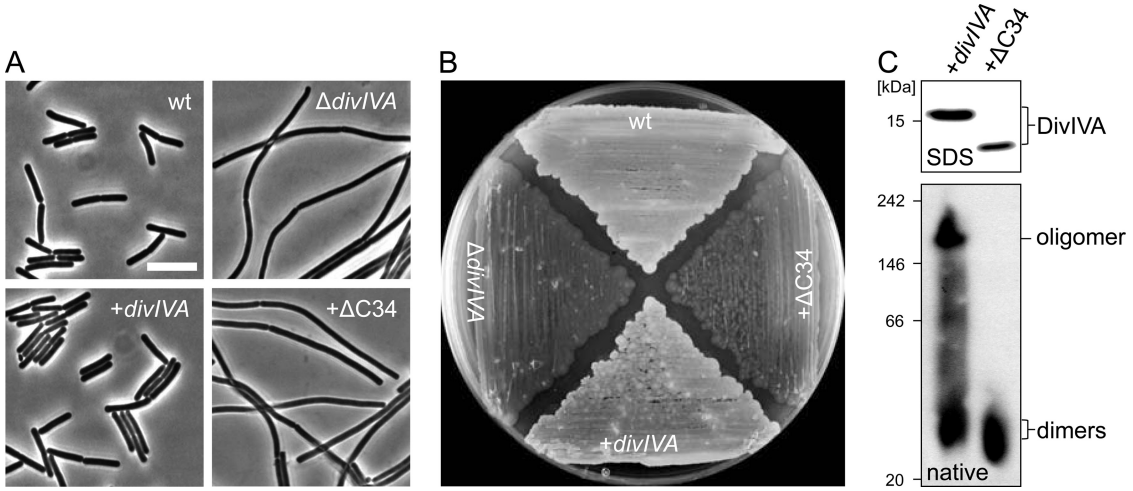

FIG 2 Complementation activity and oligomerization of a C-terminally truncated DivIVA protein devoid of the tetramerization domain. (A) Phase-contrast micrographs showing cellular morphology of strain BSN360 expressing the DivIVAΔC34 protein. Cultures of strain 168 (wt), strain 4041 (Δ*divIVA*), and the complemented Δ*divIVA* mutant strain BSN356 (+*divIVA*) were included as controls. Cells were cultivated in LB broth (containing 1 mM IPTG where necessary) to mid-logarithmic growth phase at 37°C before images were taken. Bar, 5 μm. (B) Sporulation of the same set of strains on Schaeffer's sporulation agar containing 1 mM IPTG. Cells were kept for 3 days at 37°C until lysis of the Spo$^-$ strains became apparent. (C) Western blots after SDS-PAGE and blue native PAGE to analyze expression and oligomerization of DivIVAΔC34. Strains BSN356 (+*divIVA*) and BSN360 (+ΔC34) were cultivated as described above, and cellular protein extracts were subjected to SDS-PAGE (top) or blue native PAGE (bottom) and subsequent Western blotting. DivIVA was detected using the polyclonal anti-DivIVA antiserum. The NativeMark standard (Invitrogen) was used as a molecular mass marker for blue native PAGE.

tetramerization domain and that tetramerization is a prerequisite step for octamerization.

Domain swapping to identify DivIVA interaction domains. It is possible that the C-terminal truncations used in the bacterial two-hybrid system result in misfolded and/or unstable DivIVA variants. This complicates the interpretation of the bacterial two-hybrid data. Because of this, we changed tactics and explored the possibility to swap domains between *B. subtilis* DivIVA and the closely homologous DivIVA from *L. monocytogenes*. In a previous study, we have shown that *L. monocytogenes* DivIVA displays the same localization pattern as *B. subtilis* DivIVA and is involved in SecA2-dependent protein secretion (10). *L. monocytogenes* does not sporulate and does not contain a RacA homologue. It is also unlikely that *L. monocytogenes* DivIVA interacts with MinJ, since deletion of the *divIVA* gene does not result in a minicell phenotype in *L. monocytogenes*, indicating that the listerial division site control system is DivIVA independent (10). This would enable us to separate the DivIVA domains required for localization and for RacA and MinJ interaction. First, it was necessary to confirm that *L. monocytogenes* DivIVA is normally localized when expressed in *B. subtilis*. Indeed, *L. monocytogenes* DivIVA fused to GFP and when expressed in a *divIVA*-knockout background (strain BSN373) showed a localization pattern that was similar to that of *B. subtilis* DivIVA (Fig. 3), even though *L. monocytogenes* DivIVA predominately exists as a dimer and just to a minor extent in an oligomeric form when expressed in *B. subtilis* (see Fig. S2 in the supplemental material). More importantly, however, *L. monocytogenes* DivIVA does not complement the cell division and sporulation defects of a *B. subtilis* Δ*divIVA* mutant (strain BSN238; see Fig. 5A and B). Thus, *L. monocytogenes* DivIVA seems to be unable to bind MinJ and RacA and is therefore well suited for domain swapping.

The most prominent difference between *L. monocytogenes* and *B. subtilis* DivIVA is found in the C-terminal tail (Fig. 4A), which is 11 amino acids longer in the *L. monocytogenes* protein and which has been shown to be important for binding RacA, according to the bacterial two-hybrid data. To test this, a DivIVA chimera was constructed by replacing the last 32 amino acids of *L. monocytogenes* DivIVA with the last 21 amino acids of *B. subtilis* DivIVA (*Lm*-144-*Bs* DivIVA [144 N-terminal amino acid residues of *L. monocytogenes* DivIVA fused to the corresponding C-terminal part of *B. subtilis* DivIVA; see Fig. 4A]), so that the C-terminal tails were exchanged between both proteins, whereas the core tetramerization domain (amino acids 130 to 143) was left intact (Fig. 4B). Expression of this chimera in a *B. subtilis* Δ*divIVA* background (strain BSN274) did not restore either cell division or sporulation (Fig. 5A and B). Western blotting showed that *Lm*-144-*Bs* DivIVA was stably expressed and not degraded (Fig. 4C). The chimeric protein localized normally, as a GFP fusion indicated (strain BSN295; see Fig. S4 in the supplemental material)

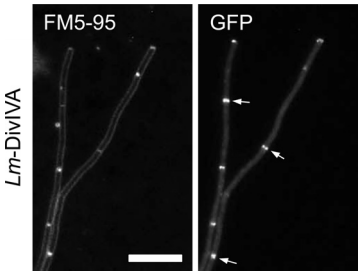

FIG 3 Localization of *L. monocytogenes* DivIVA-GFP in a *B. subtilis* Δ*divIVA* background. Strain BSN373 (expressing *L. monocytogenes* DivIVA-GFPA206K) was grown in LB medium supplemented with 0.5% xylose. The localization pattern of *L. monocytogenes* DivIVA-GFP was analyzed by epifluorescence microscopy (right), and for orientation, a FM5-95-stained image (left) was taken in parallel. Several septal DivIVA-GFP signals are indicated by arrows. Bar, 5 μm.

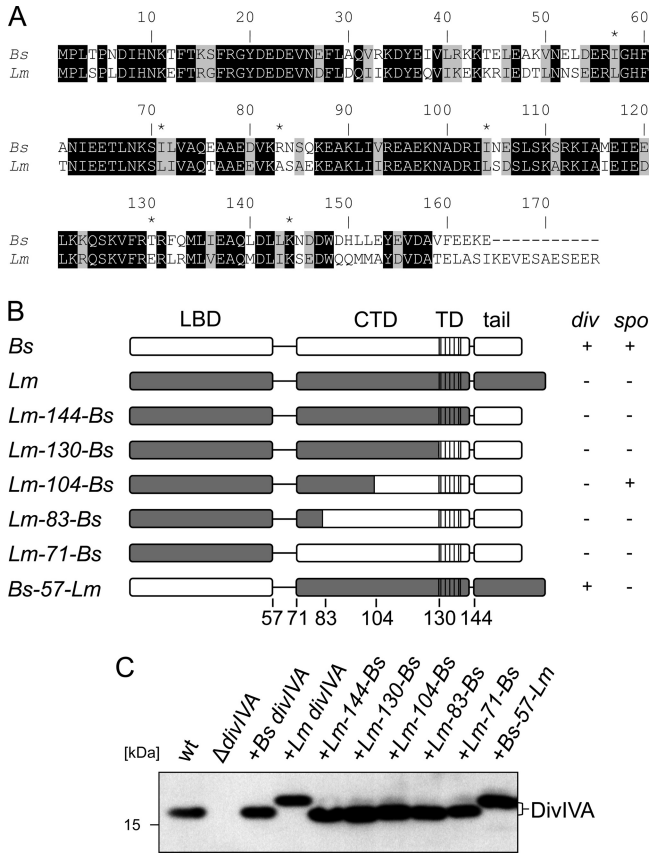

FIG 4 Expression of *L. monocytogenes* and *B. subtilis* DivIVA chimeras in *B. subtilis*. (A) Sequence alignment of the DivIVA proteins from *B. subtilis* (*Bs*) and *L. monocytogenes* (*Lm*). Identical amino acid positions are indicated by a black background, and similar amino acid positions are indicated by a gray background. The exchange sites in the different chimeras are labeled by asterisks. (B) Schematic illustration of the domain organization of the *B. subtilis* and *L. monocytogenes* DivIVA proteins and compositions of all *L. monocytogenes* and *B. subtilis* DivIVA chimeras. The abbreviations are defined in the legend to Fig. 1A. The complementation activity of the DivIVA chimeras in the complementation assays for division (*div*) and sporulation (*spo*) is indicated in the table on the right (compare Fig. 5). (C) Western blot showing expression of the DivIVA chimeras in a *B. subtilis* Δ*divIVA* background. The wild-type strain 168 and the Δ*divIVA* mutant (strain 4041), as well as strains expressing *B. subtilis divIVA* (BSN51) or *L. monocytogenes divIVA* (BSN238), were included as controls, and the DivIVA proteins were detected with an antiserum that had been raised against *B. subtilis* DivIVA (5).

and formed a stable oligomer (see Fig. S2 in the supplemental material), suggesting that the last 21 amino acids of *B. subtilis* DivIVA alone are insufficient for binding of MinJ or RacA.

Systematic domain swapping. Since MinJ and RacA binding seems to require a larger part of *B. subtilis* DivIVA, we constructed a set of chimeric DivIVA proteins in which the fusion point between the N-terminal *L. monocytogenes* and the C-terminal *B. subtilis* parts was shifted from the tail region toward the N terminus of the C-terminal domain in a stepwise fashion, as schematically indicated in Fig. 4B. Position 130 exchanged the complete C terminus beginning from the TD, positions 104 and 83 mark the beginning of short stretches in the coiled-coil region at which both proteins differ at three to four consecutive amino acid positions, whereas the domain swap at position 71 exchanged the complete C-terminal domain behind the flexible linker (Fig. 4A and B). Stability and oligomerization of the chimeras was checked by Western blotting, indicating that all the chimeric DivIVA proteins were expressed at comparable levels (Fig. 4C) and were oligomeric (see Fig. S2 in the supplemental material). Expression of these chimeras in the *B. subtilis* Δ*divIVA* background did not restore normal vegetative cell division (Fig. 5A), suggesting that they were unable to recruit MinJ. Of the different chimeras, only the *Lm*-104-*Bs* DivIVA chimera was able to restore spore formation. To confirm that the *Lm*-104-*Bs* DivIVA chimera was indeed able to recruit RacA and not MinJ, the chimera was expressed in Δ*divIVA* mutant strains containing either the GFP-RacA or the MinJ-GFP reporter. As shown in Fig. 6A and B, the *Lm*-104-*Bs* DivIVA chimera can recruit RacA but not MinJ. In conclusion, the RacA interaction domain resides in the last 60 amino acids of DivIVA and requires residues in the coiled-coil region beyond amino acid 104.

It is surprising that larger replacements of the C terminus (as in *Lm*-71-*Bs* and *Lm*-83-*Bs*) were again unable to restore sporulation. A possibility is that these chimeras did not localize properly anymore. To test this, we expressed C-terminal GFP fusions to the chimeric DivIVA constructs and analyzed their localization in *B. subtilis* Δ*divIVA* cells. Expression of all DivIVA-GFP proteins gave rise to polar and septal fluorescence signals; however, these signals occurred to different degrees (see Fig. S4A in the supplemental material). While DivIVA$^{Lm\text{-}144\text{-}Bs}$-GFP and DivIVA$^{Lm\text{-}130\text{-}Bs}$-GFP clearly accumulated at the division septa, the septal fluorescence signals of DivIVA$^{Lm\text{-}104\text{-}Bs}$-GFP, DivIVA$^{Lm\text{-}83\text{-}Bs}$-GFP, and DivIVA$^{Lm\text{-}71\text{-}Bs}$-GFP were less intense but still visible (see Fig. S4A in the supplemental material). This suggests that all DivIVA chimeras are functional in terms of lipid binding and membrane curvature sensing.

The lipid binding domain recruits MinJ. As none of the chimeras was able to complement the cell division phenotype, it may be that regions in the N-terminal domain are critical for the interaction of *B. subtilis* DivIVA with MinJ. To test this, we fused the N-terminal 57 amino acids of *B. subtilis* DivIVA spanning the entire lipid binding domain to the complete C-terminal domain of *L. monocytogenes* DivIVA (Fig. 4B). When this DivIVA chimera was expressed in a Δ*divIVA* background (strain BSN321), short cells and no minicells were observed (Fig. 5A), indicating that the *Bs*-57-*Lm* DivIVA protein recruits MinJ. The localization as well as oligomerization of this chimera is comparable to that of wild-type DivIVA (see Fig. S4 and Fig. S2 in the supplemental material, respectively) and indeed restores normal septal and polar localization of GFP-MinJ (Fig. 6A). Strikingly, sporulation was still defective in strain BSN321 (Fig. 5B) and the *Bs*-57-*Lm* chimera was unable to recruit RacA (Fig. 6B). In conclusion, the lipid binding N-terminal domain of DivIVA contains the MinJ binding site, whereas the C-terminal coiled-coil domain contains the binding site for RacA.

DISCUSSION

Here we show that two of the DivIVA interaction partners from *B. subtilis*, MinJ and RacA, bind to mutually exclusive surface regions of DivIVA. This was concluded from complementation assays with DivIVA chimeras constructed from *B. subtilis* and *L. monocytogenes* DivIVA. Analysis of a set of such DivIVA chimeras in complementation experiments surprisingly revealed that the N-terminal lipid binding domain provides the MinJ interaction module, whereas RacA binds to the C-terminal domain of

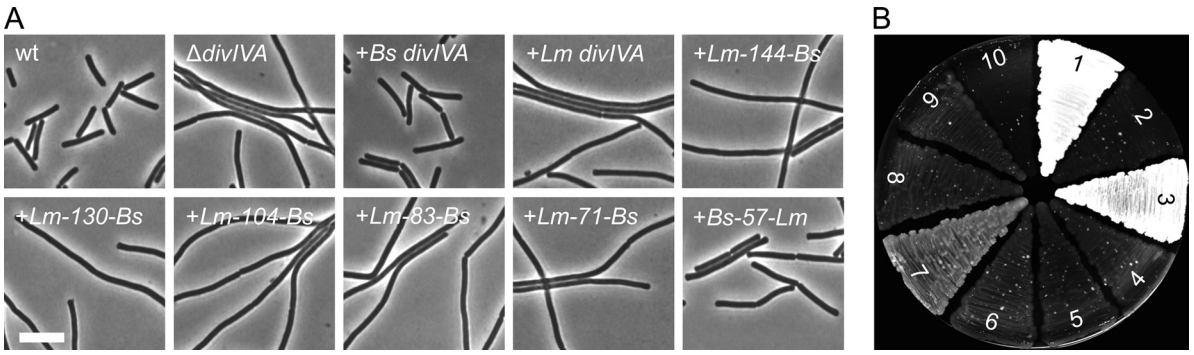

FIG 5 Complementation activity of *L. monocytogenes* and *B. subtilis* DivIVA chimeras in the *B. subtilis* Δ*divIVA* background. (A) Phase-contrast micrographs showing the ability of the tested *L. monocytogenes* and *B. subtilis* DivIVA chimeras to complement the filamentous Δ*divIVA* phenotype. Cells were cultivated in LB broth containing 0.5% xylose until mid-log growth phase at 37°C before cell morphology was assessed microscopically. Bar, 5 μm. (B) Sporulation plate assay to test the activity of the *L. monocytogenes* and *B. subtilis* DivIVA chimeras to complement the sporulation defect of the *B. subtilis* Δ*divIVA* mutant. Strains expressing the DivIVA chimeras were streaked on Schaeffer's sporulation agar containing 0.5% xylose and kept at 37°C until lysis of nonsporulating strains was comfortably distinguishable from the brownish Spo^+ strains. The wild type, the Δ*divIVA* mutant, and strains complemented with either the *B. subtilis* (BSN51) or the *L. monocytogenes* (BSN238) *divIVA* gene were used as controls. Sections: 1, strain 168 (wt); 2, strain 4041 (Δ*divIVA*); 3, strain BSN51 (*B. subtilis divIVA*); 4, strain BSN238 (*L. monocytogenes divIVA*); 5, strain BSN274 (*Lm*-144-*Bs divIVA*); 6, strain BSN278 (*Lm*-130-*Bs divIVA*); 7, strain BSN288 (*Lm*-104-*Bs divIVA*); 8, strain BSN287 (*Lm*-83-*Bs divIVA*); 9, strain BSN316 (*Lm*-71-*Bs divIVA*); 10, strain BSN321 (*Bs*-57-*Lm divIVA*). Note that sporulation of strain BSN288 (*Lm*-104-*Bs divIVA*) did not reach the wild-type level. This might be explained by the lack of MinCD activity in this strain, which is required for full sporulation (37).

DivIVA. This was unexpected since it was assumed that the C-terminal domain would constitute the protein recruitment module for both proteins, with the LBD being important only for dimerization and lipid binding. However, a dual function of the lipid binding domain is in good agreement with the two-domain nature of DivIVA proteins. The lipid binding domain is in close contact with the cytoplasmic membrane and even partially inserts into it, which makes it a good candidate for interacting with transmembrane proteins like MinJ. Since most sequence differences between the LBDs of *B. subtilis* and *L. monocytogenes* DivIVA cluster between residues E28 and I57 (Fig. 4A), this region most likely represents the MinJ binding surface of DivIVA. Support for this assumption comes from the observation that a replacement of the region from amino acids 1 to 16 of *Corynebacterium glutamicum* DivIVA by the corresponding region from *B. subtilis* DivIVA was without effect (19). Lipid binding of DivIVA via its N-terminal domain would in turn leave the C terminus free to reach into the cytoplasm. Fitting with this, our experiments indicated that the C-terminal domain is the interaction module for RacA, which is a soluble cytoplasmic protein. It was recently reported that the interaction of *C. glutamicum* ParB, which is a chromosome-binding protein like RacA, with its cognate DivIVA requires central regions of the C-terminal domain as well (9). Our results thus confirm earlier speculations that the sporulation and the division functions of DivIVA can be separated. This had been concluded from the observation that a *divIVA* mutation consisting of an N-to-D change at position 99 severely affected sporulation but not division (31). Another classical *divIVA* point mutation is the *divIVA1* mutation in which the alanine at position 78 is replaced by a threonine. This mutation causes a Div^- Spo^- phenotype (32), even though it lies outside the RacA and MinJ binding regions. Neither expression nor oligomerization of DivIVA is impaired by this mutation (33). Thus, the A78T exchange might possibly affect subcellular localization of DivIVA or induce structural changes in the protein that reduce its activity but do not influence formation of oligomers.

The question that we cannot answer conclusively is, why do the two chimeras with the more N-terminally located fusion points (*Lm*-83-*Bs* and *Lm*-71-*Bs*) not behave similarly to the *Lm*-104-*Bs* DivIVA protein? Initially, this conflicted with the idea that the C-terminal domain is the protein recruitment module for RacA, since C-terminal exchanges longer than those in *Lm*-104-*Bs* should result at least in the same degree of complementation activity. We do not think that this is explained by misfolding of the respective chimeric proteins, since they still oligomerize (see Fig. S2 in the supplemental material) and because GFP-tagged versions of these chimeras still localized to the septum to the same degree as the *Lm*-104-*Bs* GFP fusion protein (see Fig. S4A in the supplemental material) and therefore appeared to be folded properly. Moreover, a strain expressing an *Lm*-57-*Bs* DivIVA protein showed the same sporulation defect as strains expressing *Lm*-83-*Bs* and *Lm*-71-*Bs* DivIVA chimeras (data not shown). Possibly, longer C-terminal exchanges do not function in the context of an unrelated lipid binding domain. With regard to this issue, the fact that the arginine 102 residue of *B. subtilis* DivIVA is phosphorylated might be of special interest here (34). This phosphorylation could be critical for RacA recruitment and may add an extra dimension of activity control on the different DivIVA chimeras. Therefore, we constructed a phosphoablative (R102K) and a phosphomimetic (R102E) mutant allele of *divIVA* and tested their activity in our complementation system. Both of these mutations cause a Div^+ Spo^- phenotype (see Fig. S5 in the supplemental material). Hence, arginine 102 might indeed have a crucial function in RacA binding, but it is not relevant for the interaction with MinJ. Phosphorylations at the C-terminal domains are well described for DivIVA from *Mycobacterium tuberculosis* (named Wag31 in mycobacteria) and *Streptococcus pneumoniae*, even though they both occurred at threonine side chains (T73 and T201, respectively). Phenotypic analysis of phosphomimetic and phosphoablative *divIVA* mutant strains in these organisms also revealed that these phosphorylations are indeed involved in cell shape control (35, 36). In the future it will be interesting to address

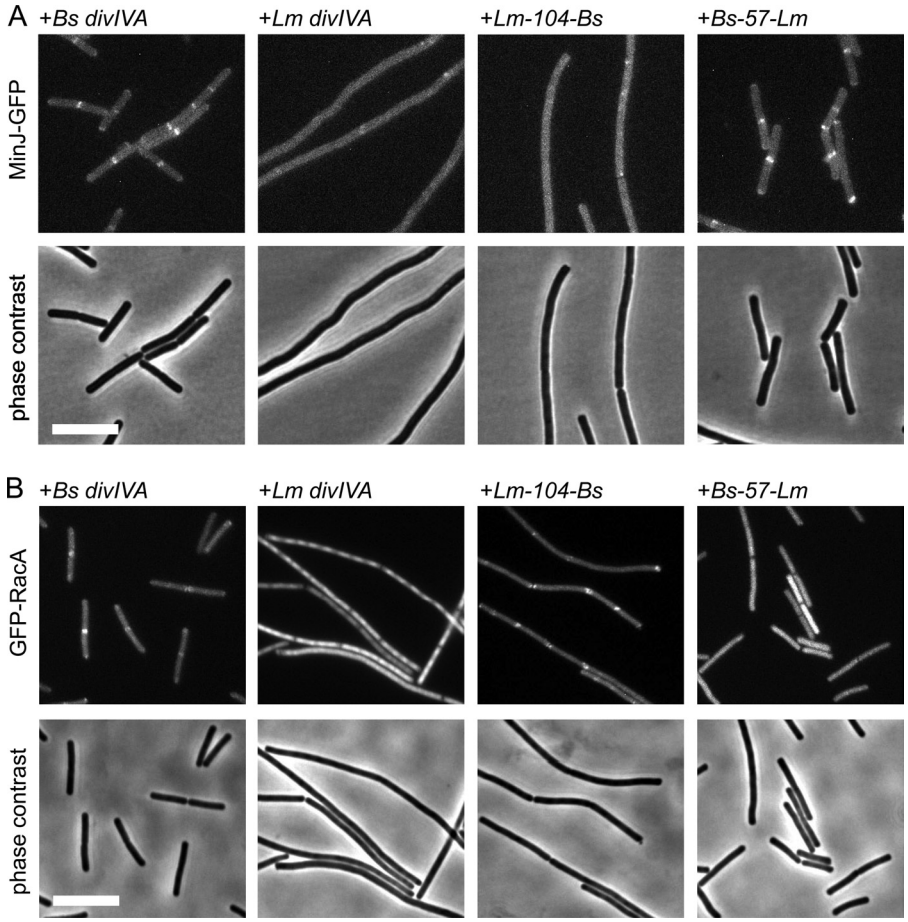

FIG 6 Localization of MinJ and RacA in *B. subtilis* strains expressing selected *L. monocytogenes* and *B. subtilis divIVA* chimeras. (A) Fluorescence micrographs showing the subcellular localization of MinJ-GFP in *L. monocytogenes* and *B. subtilis divIVA* chimera strains during mid-logarithmic growth in LB broth supplemented with 0.5% xylose at 37°C (top). MinJ-GFP was imaged in strains expressing the *Lm*-104-*Bs* DivIVA (strain BSN336) and the *Bs*-57-*Lm* DivIVA (strain BSN338) chimeras. As a control, MinJ-GFP was also visualized in Δ*divIVA* strains which express *B. subtilis divIVA* (strain BSN334) or *L. monocytogenes divIVA* (strain BSN335). Phase-contrast images were included for better orientation (bottom). (B) Localization of RacA in *B. subtilis* strains expressing the same *L. monocytogenes* and *B. subtilis divIVA* chimeras as in panel A. Fluorescence images were obtained on cells during growth in LB broth containing 0.5% xylose at 37°C (top). GFP-RacA was visualized in strains expressing the *Lm*-104-*Bs* DivIVA (strain BSN342) and *Bs*-57-*Lm* DivIVA (strain BSN344) chimeras. As controls, GFP-RacA was also imaged in strain BSN340, which expresses *B. subtilis divIVA*, and in strain BSN341, which expresses *L. monocytogenes divIVA*. Phase-contrast images were included for better orientation (bottom). Bar, 5 μm.

the regulatory impact of such phosphorylations for DivIVA binding partner recruitment.

ACKNOWLEDGMENTS

We thank Ling Juan Wu (Newcastle University) for the kind gift of the *gfp-racA* strain and Henrik Strahl (Newcastle University) for sharing plasmid pAPNC213cat.

This work was financially supported by a DAAD fellowship to K.G.K., a DFG grant (BR-2915/2-1) to M.B., and a Wellcome Trust Research Career Development Fellowship as well as a Biological Sciences Research Council Grant to L.W.H.

REFERENCES

1. **Lenarcic R, Halbedel S, Visser L, Shaw M, Wu LJ, Errington J, Marenduzzo D, Hamoen LW.** 2009. Localisation of DivIVA by targeting to negatively curved membranes. EMBO J. **28**:2272–2282.
2. **Ramamurthi KS, Losick R.** 2009. Negative membrane curvature as a cue for subcellular localization of a bacterial protein. Proc. Natl. Acad. Sci. U. S. A. **106**:13541–13545.
3. **Eswaramoorthy P, Erb ML, Gregory JA, Silverman J, Pogliano K, Pogliano J, Ramamurthi KS.** 2011. Cellular architecture mediates DivIVA ultrastructure and regulates Min activity in *Bacillus subtilis*. mBio **2**:e00257–11. 10.1128/mBio.00257-11.
4. **Edwards DH, Thomaides HB, Errington J.** 2000. Promiscuous targeting of *Bacillus subtilis* cell division protein DivIVA to division sites in *Escherichia coli* and fission yeast. EMBO J. **19**:2719–2727.
5. **Marston AL, Thomaides HB, Edwards DH, Sharpe ME, Errington J.** 1998. Polar localization of the MinD protein of *Bacillus subtilis* and its role in selection of the mid-cell division site. Genes Dev. **12**:3419–3430.
6. **Letek M, Ordonez E, Vaquera J, Margolin W, Flärdh K, Mateos LM, Gil JA.** 2008. DivIVA is required for polar growth in the MreB-lacking rod-shaped actinomycete *Corynebacterium glutamicum*. J. Bacteriol. **190**:3283–3292.
7. **Xu H, Chater KF, Deng Z, Tao M.** 2008. A cellulose synthase-like protein involved in hyphal tip growth and morphological differentiation in *Streptomyces*. J. Bacteriol. **190**:4971–4978.
8. **Wu LJ, Errington J.** 2003. RacA and the Soj-Spo0J system combine to effect polar chromosome segregation in sporulating *Bacillus subtilis*. Mol. Microbiol. **49**:1463–1475.
9. **Donovan C, Sieger B, Krämer R, Bramkamp M.** 2012. A synthetic *Escherichia coli* system identifies a conserved origin tethering factor in *Actinobacteria*. Mol. Microbiol. **84**:105–116.
10. **Halbedel S, Hahn B, Daniel RA, Flieger A.** 2012. DivIVA affects secretion

of virulence-related autolysins in *Listeria monocytogenes*. Mol. Microbiol. **83**:821–839.
11. **Bramkamp M, Emmins R, Weston L, Donovan C, Daniel RA, Errington J.** 2008. A novel component of the division-site selection system of *Bacillus subtilis* and a new mode of action for the division inhibitor MinCD. Mol. Microbiol. **70**:1556–1569.
12. **Patrick JE, Kearns DB.** 2008. MinJ (YvjD) is a topological determinant of cell division in *Bacillus subtilis*. Mol. Microbiol. **70**:1166–1179.
13. **Flärdh K.** 2003. Essential role of DivIVA in polar growth and morphogenesis in *Streptomyces coelicolor* A3(2). Mol. Microbiol. **49**:1523–1536.
14. **Kaval KG, Halbedel S.** 2012. Architecturally the same, but playing a different game: the diverse species-specific roles of DivIVA proteins. Virulence **3**:406–407.
15. **Ben-Yehuda S, Rudner DZ, Losick R.** 2003. RacA, a bacterial protein that anchors chromosomes to the cell poles. Science **299**:532–536.
16. **Briley K, Jr, Prepiak P, Dias MJ, Hahn J, Dubnau D.** 2011. Maf acts downstream of ComGA to arrest cell division in competent cells of *B. subtilis*. Mol. Microbiol. **81**:23–39.
17. **Dos Santos VT, Bisson-Filho AW, Gueiros-Filho FJ.** 2012. DivIVA-mediated polar localization of ComN, a post-transcriptional regulator of *B. subtilis*. J. Bacteriol. **194**:3661–3669.
18. **Oliva MA, Halbedel S, Freund SM, Dutow P, Leonard TA, Veprintsev DB, Hamoen LW, Löwe J.** 2010. Features critical for membrane binding revealed by DivIVA crystal structure. EMBO J. **29**:1988–2001.
19. **Letek M, Fiuza M, Ordonez E, Villadangos AF, Flärdh K, Mateos LM, Gil JA.** 2009. DivIVA uses an N-terminal conserved region and two coiled-coil domains to localize and sustain the polar growth in *Corynebacterium glutamicum*. FEMS Microbiol. Lett. **297**:110–116.
20. **Morimoto T, Loh PC, Hirai T, Asai K, Kobayashi K, Moriya S, Ogasawara N.** 2002. Six GTP-binding proteins of the Era/Obg family are essential for cell growth in *Bacillus subtilis*. Microbiology **148**:3539–3552.
21. **Lewis PJ, Marston AL.** 1999. GFP vectors for controlled expression and dual labelling of protein fusions in *Bacillus subtilis*. Gene **227**:101–110.
22. **van Baarle S, Bramkamp M.** 2010. The MinCDJ system in *Bacillus subtilis* prevents minicell formation by promoting divisome disassembly. PLoS One **5**:e9850. doi:10.1371/journal.pone.0009850.
23. **Sambrook J, Fritsch EF, Maniatis T.** 1989. Molecular cloning: a laboratory manual, 2nd ed. Cold Spring Harbor Laboratory Press, Cold Spring Harbor, NY.
24. **Zacharias DA, Violin JD, Newton AC, Tsien RY.** 2002. Partitioning of lipid-modified monomeric GFPs into membrane microdomains of live cells. Science **296**:913–916.
25. **Landgraf D, Okumus B, Chien P, Baker TA, Paulsson J.** 2012. Segregation of molecules at cell division reveals native protein localization. Nat. Methods **9**:480–482.
26. **van den Ent F, Löwe J.** 2006. RF cloning: a restriction-free method for inserting target genes into plasmids. J. Biochem. Biophys. Methods **67**:67–74.
27. **Hamoen LW, Smits WK, de Jong A, Holsappel S, Kuipers OP.** 2002. Improving the predictive value of the competence transcription factor (ComK) binding site in *Bacillus subtilis* using a genomic approach. Nucleic Acids Res. **30**:5517–5528.
28. **Karimova G, Pidoux J, Ullmann A, Ladant D.** 1998. A bacterial two-hybrid system based on a reconstituted signal transduction pathway. Proc. Natl. Acad. Sci. U. S. A. **95**:5752–5756.
29. **Harwood CR, Coxon RD, Hancock IC.** 1990. Molecular biological methods for *Bacillus*. John Wiley & Sons, Chichester, United Kingdom.
30. **Stahlberg H, Kutejova E, MuchovÁ K, Gregorini M, Lustig A, Müller SA, Olivieri V, Engel A, Wilkinson AJ, Barák I.** 2004. Oligomeric structure of the *Bacillus subtilis* cell division protein DivIVA determined by transmission electron microscopy. Mol. Microbiol. **52**:1281–1290.
31. **Thomaides HB, Freeman M, El Karoui M, Errington J.** 2001. Division site selection protein DivIVA of *Bacillus subtilis* has a second distinct function in chromosome segregation during sporulation. Genes Dev. **15**:1662–1673.
32. **Cha JH, Stewart GC.** 1997. The *divIVA* minicell locus of *Bacillus subtilis*. J. Bacteriol. **179**:1671–1683.
33. **Muchová K, Kutejova E, Scott DJ, Brannigan JA, Lewis RJ, Wilkinson AJ, Barák I.** 2002. Oligomerization of the *Bacillus subtilis* division protein DivIVA. Microbiology **148**:807–813.
34. **Elsholz AK, Turgay K, Michalik S, Hessling B, Gronau K, Oertel D, Mäder U, Bernhardt J, Becher D, Hecker M, Gerth U.** 2012. Global impact of protein arginine phosphorylation on the physiology of *Bacillus subtilis*. Proc. Natl. Acad. Sci. U. S. A. **109**:7451–7456.
35. **Kang CM, Abbott DW, Park ST, Dascher CC, Cantley LC, Husson RN.** 2005. The *Mycobacterium tuberculosis* serine/threonine kinases PknA and PknB: substrate identification and regulation of cell shape. Genes Dev. **19**:1692–1704.
36. **Fleurie A, Cluzel C, Guiral S, Freton C, Galisson F, Zanella-Cleon I, Di Guilmi AM, Grangeasse C.** 2012. Mutational dissection of the S/T-kinase StkP reveals crucial roles in cell division of *Streptococcus pneumoniae*. Mol. Microbiol. **83**:746–758.
37. **Barák I, Prepiak P, Schmeisser F.** 1998. MinCD proteins control the septation process during sporulation of *Bacillus subtilis*. J. Bacteriol. **180**:5327–5333.